analytical chemistry

pubs.acs.org/ac Article

Amplification-free Detection of Cytomegalovirus miRNA Using a Modification-free Surface Plasmon Resonance Biosensor

Ying-Feng Chang, Yi-Te Chou, Chia-Yu Cheng, Jen-Fu Hsu, Li-Chen Su,* and Ja-an Annie Ho*

Cite This: *Anal. Chem.* 2021, 93, 8002−8009 Read Online

ACCESS | Metrics & More | Article Recommendations | Supporting Information

ABSTRACT: Cytomegalovirus (CMV) is the most frequent cause of congenital infection worldwide; congenital CMV may lead to significant mortality, morbidity, or long-term sequelae, such as sensorineural hearing loss. The current study presents a newly designed surface plasmon resonance (SPR) biosensor for CMV-specific microRNAs that does not involve extra care for receptor immobilization or treatment to prevent fouling on bare gold surfaces. The modification-free approach, which utilizes a poly-adenine [poly(A)]−Au interaction, exhibited a high affinity that was comparable to that of the gold−sulfur (Au−S) interaction. In addition, magnetic nanoparticles (MNPs) were used to separate the analyte from complex sample matrixes that significantly reduced nonspecific adsorption. Moreover, the MNPs also played an important role in SPR signal amplification due to the binding-induced change in the refractive index. Our SPR biosensing platform was used successfully for the multi-detection of the microRNAs, UL22A-5p, and UL112-3p, which were associated with CMV. Our SPR biosensor offered the detection limits of 108 fM and 24 fM for UL22A-5p and UL112-3p, respectively, with an R^2 of 0.9661 and 0.9985, respectively. The precision of this biosensor has an acceptable CV (coefficient of variation) value of <10%. In addition, our sensor is capable of discriminating between serum samples collected from healthy and CMV-infected newborns. Taken together, we believe that our newly developed SPR biosensing platform is a promising alternative for the diagnosis of CMV-specific microRNA in clinical settings, and its application for the detection of other miRNAs may be extended further.

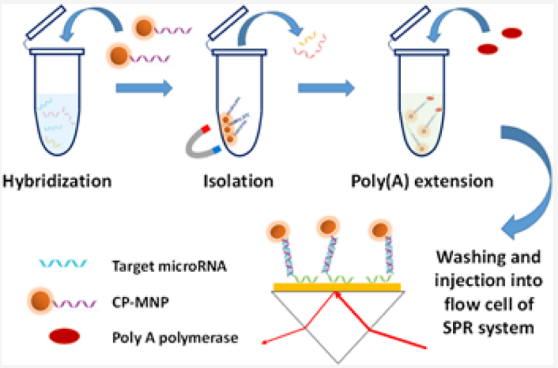

INTRODUCTION

Cytomegalovirus (CMV) is a member of the herpesviridae family, which is a double-stranded DNA virus with a diameter of about 150−200 nm. CMV is considered the most important pathogen in transplant recipient patients because it can cause significant morbidity and mortality. CMV is the most frequent cause of congenital infection worldwide; it is also the leading nongenetic cause of sensorineural hearing loss, learning difficulties,[1] and neurodevelopmental disabilities in children.[2] Approximately, 0.6−0.7% of babies are born with CMV infection;[3] however, 20% of CMV-infected babies develop symptoms of the virus or have long-term health problems. Since the earlier the baby is diagnosed, the sooner the doctor may suggest appropriate treatment,[4] suitable and applicable diagnostic tests for CMV are essential.

Clinically, there are several diagnostic methods to determine the CMV status of patients, which include serological tests for anti-CMV immunoglobulin IgM and IgG, shell vial assay, and PCR.[5] Enzyme immunoassays and indirect immunofluorescence assays are commonly used to check for the presence of anti-CMV IgM and IgG to provide evidence of recent or past infection. The shell vial assay was modified based on the traditional tube cell culture technique, in which a human fibroblast cell line was first inoculated with patient samples followed by the utilization of fluorescent monoclonal antibodies to detect viruses either directly or indirectly; this provided results within 1−3 d. Quantitative real-time polymerase chain reaction (q-PCR) is an international reference standard published by the World Health Organization (WHO) as the most commonly used method to monitor patients at the risk for CMV disease and their response to therapy. Due to variable DNA extraction procedures, the gene targets selected, and the specimen types used, the reproducibility and accuracy of the q-PCR method for CMV were somewhat inconsistent. In addition, cost ineffectiveness and lack of standardized real-time PCR protocols impeded the development of universal guidelines for the management of CMV infections.[6] Like other herpesviruses, CMV initiates gene transcription, viral DNA replication, and capsid protein expression when the physiological status of the host was suitable for virus transmission and

Received: March 12, 2021
Accepted: May 7, 2021
Published: May 24, 2021

https://doi.org/10.1021/acs.analchem.1c01093
Anal. Chem. 2021, 93, 8002−8009

replication.[7−9] During the process, CMV regulated the cellular environment of the host to complete its life cycle[10] by encoding specific microRNAs (miRNAs) that cause dysfunctional host genes.[11] Various miRNAs that are associated with CMV have been identified.[12] Among them, miR-UL22A-5p and miR-UL112-3p were found to be highly correlated with CMV infection in humans.[12−14] CMV miR-UL112-3p targeted the NK cell-activating receptor MHC, class I-related, chain B (MICB), but miR-UL22A-5p targeted autophagy-related 5 (ATG5) to modulate apoptosis.[12,15] We herein chose two CMV-specific microRNAs (miRs), UL22A-5p and UL112-3p, as model disease targets to develop a simple, modification-free, amplification-free surface plasmon resonance (SPR) biosensor.

We selected SPR as the sensing platform due to its reliability in studying biomolecular interactions; moreover, it can be developed into a real-time, sensitive diagnostic device. The detection principle of SPR is based on the excitation of surface plasmons (SPs) that are sensitive to refractive index changes caused by binding events between analytes and receptors on the metallic sensor surface, which makes SPR an excellent tool for biological detection. However, nonspecific adsorption of biomolecules, such as nontarget proteins and nucleic acids, is a major concern in SPR biosensing, especially when dealing with clinical samples. Therefore, antifouling treatment is a common procedure to diminish nonspecific interference. In the past, poly(ethylene glycol) (PEG) polymers were the most frequently used materials to prevent fouling;[16,17] however, PEG often suffered from oxidative damage in biological matrixes, which limited their use for long-term applications.[18,19] Zwitterionic polymers are an alternative antifouling material to modify the SPR sensing surface,[19−21] and they were highly resistant to nonspecific protein adsorption in complex media that were caused by the formation of an electrostatically induced hydration layer.[22,23] Regretfully, the preparation of the antifouling surface with zwitterionic polymers was complicated and required well-trained personnel. These limitations have driven researchers to find effective ways bypassing the abovementioned issues yet avoiding interference caused by the matrix of clinical samples. We believe that the exploitation of magnetic nanoparticles (MNPs) in the assay procedure may be one of the potential solutions.

MNPs have attracted attention in biosensing technology due to their superior stability, biocompatibility, and efficient isolation/concentration of analytes.[24] In particular, MNPs are capable of separating analytes from the matrix to reduce the nonspecific adsorption of an affinity biosensor,[25] which considerably upgraded SPR technology for clinical applications. Furthermore, the use of MNPs in SPR biosensors is also conducive to SPR signal amplification due to the significant changes in the binding-induced refractive index.[26] Compared with antifouling pretreatment, the application of MNPs to remove the interference and to isolate the target from the sample is a relatively simple and effective approach to avoid the matrix effect, although a receptor-modified surface is still needed to recognize the target. In addition, a poly-adenine [poly(A)] sequence was employed in the present study to demonstrate a surface modification-free strategy for SPR sensor development. Due to its high affinity for gold, the gold−poly(A) surface was comparable to the gold−sulfur (Au−S) interaction, which is the most widely engaged strategy for functionalization of a gold surface used in SPR biosensors.[27−30] Poly(A) shows the highest affinity toward gold among the homo-oligonucleotides because there are multiple binding sites chemisorbed with Au.[31−34] The poly(A) sequence has been used for electrochemical[35] or optical detection[36,37] of biomolecules, such as microRNAs (miRNAs) and messenger RNAs (mRNAs), which inspired us to advance a modification-free SPR biosensor to detect miRNAs.

Taken together, we were motivated to develop a new SPR biosensing platform for the CMV-specific microRNAs (miRs), UL22A-5p and UL112-3p. This sensing platform offers a simple, nucleic acid amplification-free, and surface modification-free strategy by integrating a MNP-assisted separation procedure and a method to generate [poly(A)]-encoding DNA sequences. This new platform technology is anticipated to discriminate between serum samples collected from healthy individuals and CMV-infected newborns effectively.

EXPERIMENTAL SECTION

Materials. The clinical serum samples were kindly provided by Dr. Jen-Fu Hsu from the Department of Neonatology, Linkou Chang Gung Memorial Hospital, Taoyuan, Taiwan (IRB no. 202001461B0). The streptavidin-labeled MNPs (50 nm) were obtained from Creative Diagnostics (Shirley, NY, USA). All the oligonucleotides were purchased from Integrated DNA Technologies (Coralville, IA, USA). The poly(A) polymerase and commercial kit for the purification of miRNAs from serum were purchased from New England Biolabs (Ipswich, MA, USA) and Qiagen (Hilden, Germany), respectively. The SYBR gold, SYBR green, and commercial qRT-PCR kits (TaqMan MicroRNA Reverse Transcription Kit, MicroRNA Assay, and Universal PCR Master Mix) for both target miRNAs, UL22A-5p and UL112-3p, were acquired from Thermo Fisher (Waltham, MA, USA). The SPR sensing chips, which were composed of an Ag−Au bimetallic layer (35/10 nm), were fabricated by Thin Film Technology Center, National Central University (Taoyuan, Taiwan).

Phosphate-buffered saline (PBS), which consisted of 137 mM NaCl, 2.7 mM KCl, and 10 mM phosphate buffer at a pH of 7.4, was used in all experiments as the working and washing buffer. Poly(A) polymerase reaction buffer (PRB, pH 7.9) that contained 50 mM Tris-HCl, 250 mM NaCl, and 10 mM $MgCl_2$ was used for the poly(A) extension process.

Conjugation of Biotinylated Capture Probes to Streptavidin-Labeled Magnetic Particles. The capture probe-sensitized magnetic particles (cp-MNP) were prepared by mixing pre-washed streptavidin-labeled MNPs (~6×10^{11} particles/mL) and 1 μM biotinylated capture probes (10:1, v/v). The reaction mixture was allowed to stand overnight at 4 °C. Finally, the prepared cp-MNPs were washed three times with PBS and re-suspended in PBS prior to use.

Target miRNA Recognition, Magnetic Isolation, and Poly(A) Extension. We mixed 10 μL of cp-MNPs (6×10^{11} particles/mL) in PBS, 1 μL of 3% Triton X-100, and 20 μL of sample solution (either clinical samples or synthetic target miRNA in PBS) to permit the recognition of target microRNA. This reaction was continued for 30 min, which allowed target miRNAs to hybridize with the capture probe on cp-MNPs. After five cycles of washing, the target miRNA-attached cp-MNPs were isolated from the reaction mixture with a magnet followed by re-suspension in 7.5 μL of PBS. Subsequently, 1 μL of 10 mM ATP, 1 μL of 10× PRB, and 0.5 μL of 2.5 U/μL poly A polymerase, which is a template-independent enzyme, were added to the purified miRNA-attached cp-MNPs (7.5 μL) to make up a 10 μL reaction solution. The elongation of poly(A)-encoding DNA sequences was achieved by allowing

https://doi.org/10.1021/acs.analchem.1c01093
Anal. Chem. 2021, 93, 8002−8009

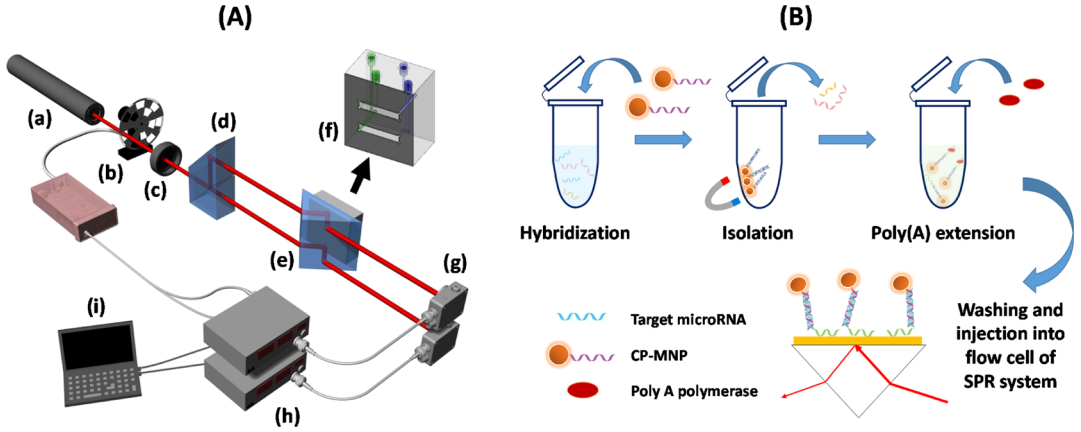

Figure 1. Schematic illustration of a modification-free, nucleic acid amplification-free surface, plasmon resonance-based biosensor for the detection of cytomegalovirus miRNA. (A) Configuration of the homemade SPR biosensing system. (a) He−Ne laser, (b) optical chopper, (c) polarizer, (d) displacement beam splitter, (e) prism, (f) flow cell, (g) optical detectors, (h) lock-in amplifiers, and (i) notebook computer. (B) Schematic description of the sensing scheme.

the reaction mixture to progress for another 15 min at 37 °C, which enabled the transfer of adenosine residues from ATP to the 3′-end of target microRNA that hybridized on cp-MNPs. Finally, the elongation of the poly(A) tail was stopped by an addition of 1 μL of 110 mM EDTA. After washing three times, the reaction mixture was diluted to 500 μL with PBS and injected into the flow cell of a homemade SPR biosensing system.

Optical Setup of the SPR System and Its Performance for the Measurement of Target miRNAs. The optical setup of the homemade SPR biosensing system included a helium/neon laser (He−Ne laser, Thorlabs, Newton, NY, USA) to emit red light with a wavelength of 633 nm, and the light was allowed to pass through an optical chopper (Stanford Research Systems, Sunnyvale, CA, USA) to modulate the intensity at a frequency of 1 kHz (Figure 1A). The intensity-modulated light source was beneficial to filter out the DC background noise.[38] A polarizer was used to produce p-polarized light. Moreover, a lateral displacement beamsplitter precisely split a p-polarized input light beam into two parallel beams that were subsequently incident into the homemade dual-channel SPR device at a fixed angle. Two lock-in amplifiers (Stanford Research Systems, Sunnyvale, CA, USA) were included for simultaneous measurement of the amplitudes of reflected light beams from the reference and signal channels. The reference channel was infused with PBS solution, and the signal channel was filled with a reaction mixture that contained variable concentrations of target miRNAs prepared as described in the section Target miRNA Recognition, Magnetic Isolation, and Poly(A) Extension. The mixture product, poly(A)-tailed miRNA-attached cp-MNPs, adsorbed directly onto the bare gold surface of the SPR sensing chip, which resulted in refractive index changes in the sensing region and a subsequent change in the signal. A chemical surface pre-treatment was no longer necessary for our sensor design. The output of the signal channel was divided by that of the reference channel to obtain a normalized SPR signal. Our data processing method permitted a reduction in the disturbances that arise from laser intensity noise and any variation caused by the quality of the gold sensing surface.

Quantification of UL22A-5p and UL112-3p Using TaqMan MicroRNA Assays. Samples required for performing quantitative reverse transcription polymerase chain reaction (qRT-PCR) assays included the purified cell-free total RNA from serum and the synthetic target miRNAs in PBS. qRT-PCR was conducted using TaqMan MicroRNA assays according to the manufacturer's protocol. First, 0.15 μL of 100 mM dNTPs, 1 μL of 50 U/μL RT enzyme, 1.5 μL of 10× RT buffer, 0.19 μL of 20 U/μL of RNase inhibitor, and 4.16 μL of ddH_2O were mixed for a total of 7 μL of reaction volume. A total of 5 μL of the sample solution was added to the mixture, and 3 μL of RT primer was introduced subsequently as well. The reverse transcription was performed at 16 °C for 30 min, 42 °C for 30 min, and 85 °C for 5 s, with the final cooling at 4 °C. Second, PCR reactions were carried out in a total volume of 20 μL that contained 1.33 μL of product from the RT reaction, 1 μL of TaqMan microRNA assay, 10 μL of TaqMan universal PCR Master Mix, and 7.67 μL of ddH_2O. Finally, thermal cycling conditions were set for 10 min at 95 °C for enzyme activation followed by 40 cycles (95 °C for 15 s and 60 °C for 60 s) for amplification.

RESULTS AND DISCUSSION

Principle of the Detection Scheme. A schematic representation of the amplification-free, modification-free SPR system to detect miRNAs shows that the assay consisted of three components, which included (1) a magnetic isolation of target miRNAs, (2) a [poly(A)] extension, and (3) an acquisition of the SPR signal readout (Figure 1B). In brief, the pre-prepared cp-MNPs were first mixed with samples and allowed to hybridize with target miRNAs followed by magnetic separation. The purification through magnetic separation enabled the subsequent isolation of the target miRNAs from a complicated sample matrix to avoid nonspecific adsorption to the sensing surface, which was the leading issue that affected the performance of affinity biosensors.[6,39] Moreover, MNPs amplified the binding-induced SPR significantly, which led to an improvement in the detection limit below the pM level.[10,40−42] The size of MNPs used here was 50 nm, which has been reported previously to promote a great enhancement in SPR response without affecting the biomolecular binding efficiency.[43] Next, poly(A) polymerase was used to add a long tail of adenine nucleotides at the 3′ end of the target miRNA that hybridized with the capture probe on MNPs. A poly(A) extension enabled an effective adsorption of the miRNA on the SPR sensing chip, which was attributed to the high affinity

https://doi.org/10.1021/acs.analchem.1c01093
Anal. Chem. 2021, 93, 8002−8009

Table 1. Characterization of Poly(A) Extension by a Zetasizer Using the Techniques of Dynamic Light Scattering (DLS) and Electrophoretic Light Scattering[a]

sample	Z-average (nm)	zeta potential (mV)	PDI
control group (cp-MNPs only)	124.8 ± 1.1	−12.0 ± 0.79	0.108
experimental group (miRNA-cp-MNP complexes)	434.6 ± 31.46	−15.3 ± 1.9	0.509

[a]Z-average: the intensity-weighted mean hydrodynamic size. PDI: polydispersity index from DLS measurements.

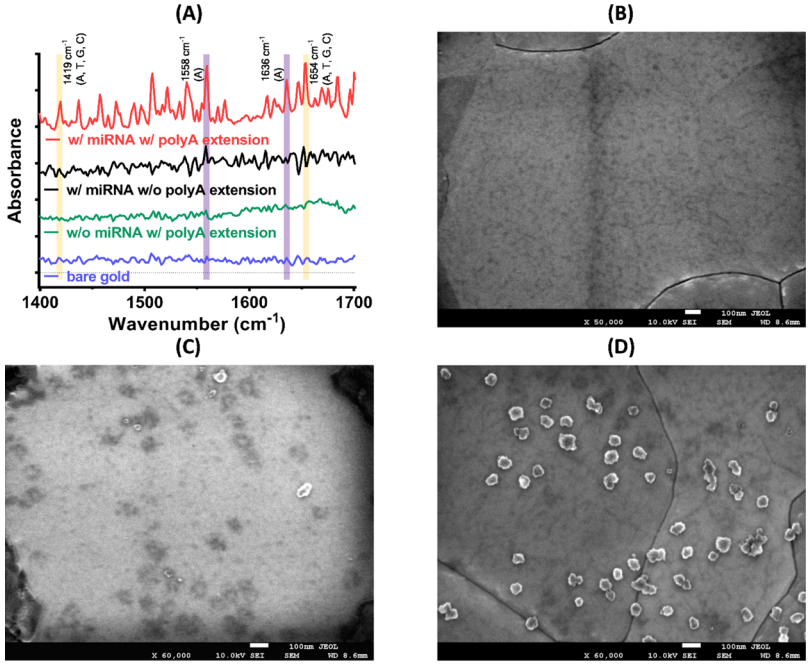

Figure 2. Characterization of the formation of [poly(A)]-miRNA-cp-MNP complexes induced by the presence of target miRNAs. Experimental sample solution (that contained synthetic target miRNA) and blank sample solution (that contained no target miRNA sequences) were subjected to go through the target probe hybridization, magnetic isolation, and [poly(A)] extension. The FTIR spectra of the bare gold surface for blank (blue), control (gold surface reacted with the blank sample, designated as green), experimental 1 (miRNA-cp-MNP complexes without poly(A) extension, designated as black), and experimental 2 (miRNA-cp-MNP complexes with poly(A) extension, designated as red) samples. The SEM images of (B) bare gold surface, (C) gold surface after reacting with the blank sample, and (D) experimental sample containing synthetic target miRNA. cp-MNP represents the capture probe streptavidin-labeled MNP.

between the adenines of the poly(A) sequences and gold.[16,17,20] In addition, the poly(A) tail triggered a huge change in the refractive index in the evanescent field of the SPR sensing surface, which led to the intensification of the SPR response. After an addition of EDTA to stop the poly(A) extension and a follow-up washing, the signal acquisition was done by injecting the solution that contained the poly(A)-extended, target miRNA-cp-MNP complex ([poly(A)]-miRNA-cp-MNP) into the flow cell of a home-made SPR system.

Characterization of Poly(A) Extension. A zetasizer (Malvern, Westborough, MA, USA) was used to confirm the extension of poly(A). The control and experimental samples that contained cp-MNPs (~1.2×10^9 particles/mL) only and miRNA-cp-MNP complexes (~1.2×10^9 particles/mL), respectively, underwent the nucleic acid hybridization, magnetic isolation, and poly(A) extension sequentially as described in the previous section. By the end of the reaction process, the hydrodynamic diameters of 124.8 ± 1.1 and 434.6 ± 31.46 nm were obtained for the control and experimental sample, respectively. Furthermore, the zeta potential of control and experimental samples was measured as −12.0 ± 0.79 and −15.3. ± 1.9 mV, respectively. The changes in the size and zeta potential indicated that a long poly(A) tail was extended onto miRNA. Table 1 shows the size distribution and zeta potential of various samples. Intensity-weighted distributions and number-weighted distributions for cp-MNPs and for miRNA-cp-MNPs are shown in Figure S1.

Characterization of the Gold Surface before and after miRNA-Poly(A) Adsorption. To confirm the successful adsorption of [poly(A)]-miRNA-cp-MNP complexes onto the gold surface using the poly(A) tail, a Fourier transform infrared (FTIR) spectrometer (Bruker, Billerica, MA, USA) and a Schottky field emission scanning electron microscope (JEOL, Tokyo, Japan) were used. The control (w/o miRNA-112) and experimental sample (w/100 nM of miRNA-112) that contained cp-MNPs (6×10^{11} particles/mL) underwent various reaction combination (the nucleic acid hybridization, magnetic isolation, and poly(A) extension) as described in the previous section. Figure 2A shows the FTIR spectra of the bare gold surface for blank (blue), control (green), experimental 1 (black), and experimental 2 (red) samples. Remarkable differences were observed among FTIR spectra that were obtained for experimental and control samples due to the formation of [poly(A)]-miRNA-cp-MNPs and their adsorption onto the gold surface. Several common IR bands were recognized in the FTIR vibrational spectra because nucleic acids showed characteristic absorbances at 1419 and 1654

https://doi.org/10.1021/acs.analchem.1c01093
Anal. Chem. 2021, 93, 8002−8009

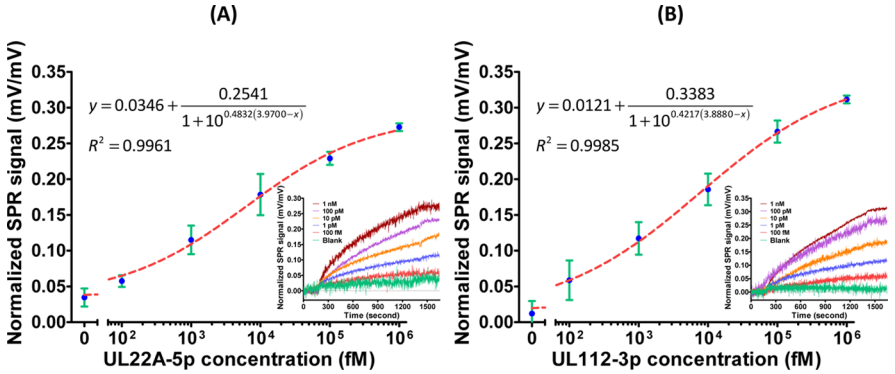

Figure 3. Dose−response curves for the CMV-associated miRNAs, (A) UL22A-5p and (B) UL112-3p. Correlation between the normalized SPR signal and the concentration of the miRNAs existing in PBS was over the range from 100 fM to 1 nM. The dynamic SPR signals for various concentrations of both target miRNAs in PBS are shown in the insets of the figure.

cm^{-1} (yellow zone); in addition, the bands at 1558 and 1636 cm^{-1} (purple zone in Figure 2A) were attributed to the presence of adenine bases.[16] Moreover, the characteristic peaks of the streptavidin-labeled MNPs are noted around 1450−1550 cm^{-1}.[44,45] Some other small peaks appearing in the range of 1400−1600 cm^{-1} (i.e., 1492, 1529, and 1579 cm^{-1})[46,47] were previously reported for nucleic acids. The scanning electron microscopy (SEM) images of three gold surfaces that reacted with blank, control, and experimental samples were taken. MNPs were positioned randomly on the gold surface (Figure 2D), but no MNPs are observed in Figure 2B,C. These results confirmed that only the [poly(A)]-miRNA-cp-MNPs appeared to adsorb onto the gold surface using poly(A) tails.

Optimization of Experimental Conditions. For our sensor format, the detection sensitivity would have been influenced if one cp-MNP hybridized with more than one target miRNA molecule. To avoid this situation, we can either optimize the conjugation of biotinylated capture probes to streptavidin-labeled MNPs to ensure that only one capture probe was modified on one MNP or we could adjust the number of cp-MNPs to make the Poisson probability of observing the hybridization of a single cp-MNP with >1 target miRNA molecule negligibly small. For example, if ca. 6×10^9 cp-MNPs were allowed to interact with the sample solution that contained the CMV-related miRNAs, UL22A-5p and UL112-3p, in the range of 10^3 to 10^7 copies,[48] the calculated probability for each cp-MNP that hybridized with >1 target miRNA molecule would range from 10^{-4} to 10^{-11}% based on the definition of the Poisson distribution. Therefore, with our optimized experimental conditions, most of the cp-MNPs hybridized with only one target miRNA molecule, which led to the best assay performance.

A poly(A) extension is the other imperative element that affected the sensing performance of the current detection scheme. Poly(A) polymerase plays a key role in the poly(A) extension process, and therefore, it was essential to optimize the concentration of poly(A) polymerase and the reaction time for the ideal performance of the assay. Experimentally, cp-MNP solution and 1 nM target miRNA were first mixed to initiate the recognition for 30 min. After a washing step, various poly(A) polymerase concentrations (0, 0.05, 0.125, 0.25, and 0.5 U/μL) were used to decide the efficient poly(A) extension at 37 °C. Fluorescence kinetics of SYBR gold was acquired using qPCR (Bio-Rad, Hercules, CA, USA). A maximal relative fluorescence unit (RFU) of ∼140 was observed at a concentration of 0.25 U/μL, and no significant increase in the RFU was found thereafter (Figure S2A). In addition, the fluorescence increased with reaction time, but no further significant changes in the generated RFU occurred after 900 s (Figure S2A). For the observation outlined above, the optimal poly(A) polymerase concentration and reaction time for the poly(A) extension process were 0.25 U/μL and 900 s, respectively.

Detection Specificity of Our Assay. The detection specificity (or selectivity) is vital for a bioassay, and the selectivity of the proposed detection scheme was solely dependent on the recognition specificity of cp-MNPs designed herein. Fortunately, the target miRNAs were encoded by CMV, which meant that there was no homologous miRNA presented in the non-CMV-infected biological samples that were collected from humans. Accordingly, we anticipated that only UL22A-5p and UL112-3p were specifically isolated by cp-MNPs. Moreover, we chose three frequently studied disease-associated miRNAs (miR-21, miR-let-7a, and miR-221) to further confirm the cross-reactivity of our cp-MNPs. Experimentally, cp-MNPs were mixed with five testing solutions of 1 nM concentration that contained miR-21, miR-let-7a, miR-221, UL22A-5p, and UL112-3p, and they were allowed to react for 30 min to initiate hybridization. After the poly(A) extension and a washing step, the kinetic fluorescence signal of SYBR gold was acquired under the optimal conditions as described above. Only two target miRNAs, UL22A-5p and UL112-3p, were recognized and isolated by cp-MNPs, followed by the formation of a poly(A) tail, which was evidenced by the rising fluorescence signals (Figure S2B). In contrast, no increment in fluorescence signals was found in the three nontarget controls, where the acquired fluorescent signals were similar to those of the blank test. This result implied that the recognition specificity of cp-MNPs was robust, and no cross-reactivity was observed with our cp-MNPs.

Assay Performance. The optimal conditions to carry out a poly(A) extension, together with an ideal number of cp-MNPs, facilitated a specific and sensitive detection of the target miRNAs. The successful translation of [poly(A)]-miRNA-cp-MNP input to the SPR exhibited a calibration curve that showed a normalized SPR response against the concentrations of UL22A-5p and UL112-3p, in the range from 100 fM to 1 nM. Responses obtained from the signal channel were normalized to those of the reference channel. The normalized SPR signal that resulted increased as the concentration of the target miRNA increased (Figure 3). A positive correlation

https://doi.org/10.1021/acs.analchem.1c01093
Anal. Chem. 2021, 93, 8002−8009

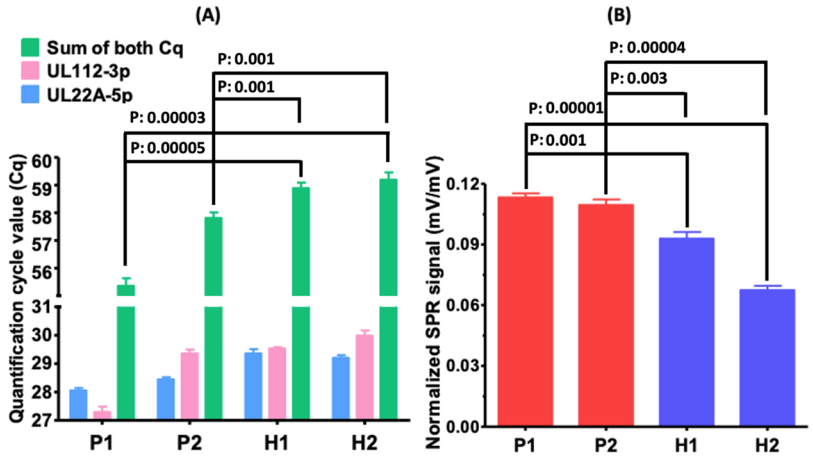

Figure 4. Real sample analysis and its validation with qPCR [samples from two healthy newborns (H1 and H2) and newborns with CMV infection (P1 and P2)]. Results obtained using (A) commercial qRT-PCR kit and (B) newly developed SPR biosensing platform.

meant that the more target miRNA molecules there were, the more [poly(A)]-miRNA-cp-MNP complexes were formed and adsorbed onto the gold sensing surface through the poly(A) tails. Finally, the obtained dose−response curves were made to fit a four-parameter, nonlinear regression, like many other SPR-based biosensors.[2,49,50] The coefficient of determination, *R*-square (R^2), of the four-parameter, dose−response curve for both target miRNAs, UL22A-5p and UL112-3p, was 0.9961 and 0.9985, respectively. According to the IUPAC definition, the limit of detections and the limit of quantification were defined as three times and ten times the standard deviation of the mean of blank determinations, respectively, which were calculated to be 108 fM and 3 pM for UL22A-5p, respectively, and 24 fM and 740 fM for UL112-3p, respectively. The dynamic range for UL22A-5p and UL112-3p was determined to be from 0.1 pM to 1 nM, covering about 4 orders of magnitude, and from 0.01 pM to 1 nM for UL112-3p, covering about 5 orders of magnitude. In addition, Figure 3 shows linearity over 3 orders of magnitude for both targets (from pM to nM) and a coefficient of variation of <10%, confirming that the precision/repeatability of this biosensor is acceptable. The dynamic SPR responses for various concentrations of both target miRNAs in PBS buffer are shown in the insets of Figure 3A,B.

Real Sample Detection. To validate the bioapplicability of our new SPR biosensing platform toward the microRNA detection in clinical specimens, sera from four newborns (two newborns with CMV infection and two healthy newborns) were collected and analyzed. In addition, a commercial qRT-PCR kit was used in parallel to validate these four serum samples. Statistically significant differences in the value of the quantification cycle (C_q), the PCR cycle number at which the reaction curve intersects the threshold line, for both UL22A-5p and UL112-3p were found among the serum samples of CMV-infected newborn #1 (P1) and two healthy controls (H1 and H2) (Figure 4A). More specifically, it meant that the levels of UL22A-5p and UL112-3p in the P1 serum sample were much higher than those in the H1 and H2 serum samples. As for the serum sample of CMV-infected newborn #2 (P2), we observed a difference in the C_q value for the miRNA UL22A-5p compared with those in two healthy controls, that is, only UL22A-5p was found to be elevated in the P2 serum sample. After we summed up two C_q values for each serum sample, it was possible to discriminate CMV-infected newborns from healthy ones (as seen in Figure 4A).

On the contrary, for SPR analyses, two cp-MNPs designed for UL22A-5p and UL112-3p were mixed in equal portions with Triton X-100 (1 μL) and a serum sample (20 μL) to initiate recognition of target miRNAs, magnetic isolation, and poly(A) extensions, as described in the previous section; the resulting reaction mixture was injected subsequently into the homemade SPR biosensing system. The output SPR signal was due to the recognition of two target miRNAs simultaneously and accumulatively, rather than individually and separately. The results indicated that the CMV-infected and healthy newborns were distinguishable by our newly developed SPR system (Figure 4B).

A summary (Table S1) of the detection characteristics of recent SPR-based biosensing platforms for miRNA detection[5,51−53] and our current method revealed that no significant differences (0.2−1.5 pM) in sensitivity were found among these SPR-based platforms because all the methods employed similar amplification techniques: strand displacement amplification and catalytic hairpin assembly and comparable SPR signal enhancement strategies involving the utilization of streptavidin or nanoparticles, such as gold nanoparticles and MNPs. Our sensor platform offered reasonable analysis time per assay (<1 h), which was comparable to that of the SPR sensor developed by Homola's group (2015). Furthermore, a comparison table (Table S2) of our SPR biosensing platform with the conventional qPCR revealed that the proposed SPR sensor platform was cost-effective and user-friendly. Moreover, an antifouling surface modification was employed by Homola's group, but our sensing platform required only magnetic isolation to eliminate undesired adsorption rather than a tedious antifouling modification.

CONCLUSIONS

As a leading cause of congenital infections worldwide, congenital CMV (cCMV) is considered to be a global public health issue. However, currently, there is no universal program that offers neonatal screening to identify infected newborns.[54,55] The lack of adequate sensitivity, specificity, and cost effectiveness may be of major concern. We herein developed and demonstrated a simple, nucleic acid amplification-free, and surface modification-free strategy for miRNA detection using a SPR biosensing platform that integrated

https://doi.org/10.1021/acs.analchem.1c01093
Anal. Chem. 2021, 93, 8002−8009

magnetic separation and poly(A) extension. The utilization of the cp-MNPs permitted recognition and isolation of target miRNAs to significantly reduce nonspecific adsorption. Moreover, the MNPs also played a vital role in strengthening the binding-induced SPR response to empower a substantial improvement in the detection sensitivity to the picomolar (pM) level. Subsequently, the target miRNAs that hybridized with cp-MNPs were further elongated with poly(A) sequences using the utility of poly(A) polymerase. Due to the superb affinity of poly-adenine for gold, the extended poly(A) tail was capable of specifically adsorbing onto the SPR gold sensing surface to allow the signal translation from a miRNA recognition event to a SPR readout for the detection of target miRNAs. Our current SPR platform approach offers a sensitive detection for the CMV-associated miRNAs, UL22A-5p and UL112-3p, with a detection limit of 1.55 and 0.54 pM, respectively, based on the IUPAC definition. In addition, serum samples from four newborns were tested using our SPR platform, which distinguished among healthy and CMV-infected newborns within 1 h. The results were in agreement with those obtained from a commercial qRT-PCR kit. Our findings implied that the miRNAs, UL22A-5p and UL112-3p, that were selected as targets in our study have a great diagnostic potential for detecting cytomegalovirus, and our newly developed SPR biosensing platform is a prospective analytical method for multi-miRNA detection in clinical applications.

■ ASSOCIATED CONTENT

Supporting Information

The Supporting Information is available free of charge at https://pubs.acs.org/doi/10.1021/acs.analchem.1c01093.

> Comparison of the proposed SPR biosensing platform and the recent SPR-based sensors, performance and specificity of our probing system, optimization of the poly(A) polymerase concentration, reaction time for the poly(A) extension procedure performed at 37 °C, kinetic plots of accumulated poly(A) products using various concentrations of poly(A) polymerase (0, 0.05, 0.125, 0.25, and 0.5 U/μL), and specificity of the cp-MNPs toward two targets, UL22A-5p and UL112-3p, and three commonly studied miRNAs (miR-221, miR-let71, and miR-21) (PDF)

■ AUTHOR INFORMATION

Corresponding Authors

Li-Chen Su − *General Education Center and Organic Electronics Research Center, Ming Chi University of Technology, New Taipei City 24301, Taiwan;* orcid.org/0000-0003-0731-3758; Phone: +886-2-29089899#4533; Email: sulichen@o365.mcut.edu.tw

Ja-an Annie Ho − *BioAnalytical Chemistry and Nanobiomedicine Laboratory, Department of Biochemical Science and Technology and Department of Chemistry, National Taiwan University, Taipei 10617, Taiwan; Center for Emerging Materials and Advanced Devices and Center for Biotechnology, National Taiwan University, Taipei 10617, Taiwan;* orcid.org/0000-0001-6684-1118; Phone: +886-2-33664438; Email: jaho@ntu.edu.tw

Authors

Ying-Feng Chang − *BioAnalytical Chemistry and Nanobiomedicine Laboratory, Department of Biochemical Science and Technology, National Taiwan University, Taipei 10617, Taiwan; Artificial Intelligence Research Center, Chang Gung University, Taoyuan 33302, Taiwan*

Yi-Te Chou − *BioAnalytical Chemistry and Nanobiomedicine Laboratory, Department of Biochemical Science and Technology, National Taiwan University, Taipei 10617, Taiwan*

Chia-Yu Cheng − *BioAnalytical Chemistry and Nanobiomedicine Laboratory, Department of Biochemical Science and Technology, National Taiwan University, Taipei 10617, Taiwan*

Jen-Fu Hsu − *Division of Pediatric Neonatology, Department of Pediatrics, Linkou Chang Gung Memorial Hospital, Taoyuan 33305, Taiwan; College of Medicine, Chang Gung University, Taoyuan 33302, Taiwan*

Complete contact information is available at: https://pubs.acs.org/10.1021/acs.analchem.1c01093

Author Contributions

Y.-F.C., Y.-T.C., C.-Y.C., and J.-F.H. contributed equally to this work. Y.-F.C., C.-Y.C., and L.-C.S designed the sensor scheme and took part in data interpretation, and C.-Y.C. performed the experiments. Y.-T.C. took part in particle characterization, sensor validation, and data interpretation. J.-F.H. was responsible for IRB application, collection of clinical samples, and sensor validation. J.-a.-A.H. supervised the sensor development part and also the clinical sample validation part of the project. All authors participated in the writing of the manuscript. All authors discussed the results and implications and commented on the manuscript at all stages. The majority of this work was performed while Y.-F.C. and L.-C.S. were with National Taiwan University and Chinese Culture University, respectively.

Notes

The authors declare no competing financial interest.

■ ACKNOWLEDGMENTS

The authors gratefully acknowledge the financial support from the Ministry of Education of Taiwan and Ministry of Science and Technology under Grants nos. 106-2113-M-002-014-MY3 (Ho), 106-2622-M-002-003-CC2 (Ho), 107-2622-M-002-001-CC2 (Ho), MOST-106 -2811-M-002-099 (Ho), and MOST 108-2112-M-034-001-MY3 (Su). The authors also thank the Instrumentation Center of National Taiwan University for assistance in obtaining SEM images.

■ REFERENCES

(1) Kawano, Y.; Kawada, J.; Kamiya, Y.; Suzuki, M.; Torii, Y.; Kimura, H.; Ito, Y. *J. Perinatol.* **2016**, *36*, 1101−1105.
(2) Marsico, C.; Kimberlin, D. W. *Ital. J. Pediatr.* **2017**, *43*, 38.
(3) Cannon, M. J. *J. Clin. Virol.* **2009**, *46*, S6−S10.
(4) Carlson, A.; Norwitz, E. R.; Stiller, R. J. *Rev. Obstet. Gynecol.* **2010**, *3*, 172−179.
(5) Saldan, A.; Forner, G.; Mengoli, C.; Gussetti, N.; Palù, G.; Abate, D. *J. Clin. Microbiol.* **2017**, *55*, 693−702.
(6) Ross, S. A.; Novak, Z.; Pati, S.; Boppana, S. B. *Infect. Disord.: Drug Targets* **2011**, *11*, 466−474.
(7) Sinzger, C.; Digel, M.; Jahn, G. *Curr. Top. Microbiol. Immunol.* **2008**, *325*, 63−83.

(8) Ogawa-Goto, K.; Tanaka, K.; Gibson, W.; Moriishi, E.; Miura, Y.; Kurata, T.; Irie, S.; Sata, T. *J. Virol.* **2003**, *77*, 8541−8547.
(9) Gibson, W. *Curr. Top. Microbiol. Immunol.* **2008**, *325*, 187−204.
(10) Hook, L. M.; Grey, F.; Grabski, R.; Tirabassi, R.; Doyle, T.; Hancock, M.; Landais, I.; Jeng, S.; McWeeney, S.; Britt, W.; Nelson, J. A. *Cell Host Microbe* **2014**, *15*, 363−373.
(11) Filipowicz, W.; Bhattacharyya, S. N.; Sonenberg, N. *Nat. Rev. Genet.* **2008**, *9*, 102−114.
(12) Zhang, L.; Yu, J.; Liu, Z. *Virol. J.* **2020**, *17*, 34.
(13) Lisboa, L. F.; Egli, A.; O'Shea, D.; Åsberg, A.; Hartmann, A.; Rollag, H.; Pang, X. L.; Tyrrell, D. L.; Kumar, D.; Humar, A. *Am. J. Transplant.* **2015**, *15*, 1893−1902.
(14) Landais, I.; Pelton, C.; Streblow, D.; DeFilippis, V.; McWeeney, S.; Nelson, J. A. *PLoS Pathog.* **2015**, *11*, No. e1004881.
(15) Kim, S.; Seo, D.; Kim, D.; Hong, Y.; Chang, H.; Baek, D.; Kim, V. N.; Lee, S.; Ahn, K. *Cell Host Microbe* **2015**, *17*, 838−851.
(16) Liu, B.; Liu, X.; Shi, S.; Huang, R.; Su, R.; Qi, W.; He, Z. *Acta Biomater.* **2016**, *40*, 100−118.
(17) Castiello, F. R.; Tabrizian, M. *Anal. Chem.* **2018**, *90*, 3132−3139.
(18) Jiang, S.; Cao, Z. *Adv. Mater.* **2010**, *22*, 920−932.
(19) Vaisocherová, H.; Yang, W.; Zhang, Z.; Cao, Z.; Cheng, G.; Piliarik, M.; Homola, J.; Jiang, S. *Anal. Chem.* **2008**, *80*, 7894−7901.
(20) Vaisocherová, H.; Šípová, H.; Víšová, I.; Bocková, M.; Špringer, T.; Laura Ermini, M.; Song, X.; Krejčík, Z.; Chrastinová, L.; Pastva, O.; Pimková, K.; Dostálová Merkerová, M.; Dyr, J. E.; Homola, J. *Biosens. Bioelectron.* **2015**, *70*, 226−231.
(21) Vaisocherová-Lísalová, H.; Víšová, I.; Ermini, M. L.; Špringer, T.; Song, X. C.; Mrázek, J.; Lamačová, J.; Scott Lynn, N., Jr.; Šedivák, P.; Homola, J. *Biosens. Bioelectron.* **2016**, *80*, 84−90.
(22) Shao, Q.; Jiang, S. *Adv. Mater.* **2015**, *27*, 15−26.
(23) Mi, L.; Jiang, S. *Angew. Chem., Int. Ed.* **2014**, *53*, 1746−1754.
(24) Sun, Y.; Bai, Y.; Song, D.; Li, X.; Wang, L.; Zhang, H. *Biosens. Bioelectron.* **2007**, *23*, 473−478.
(25) Wang, Y.; Dostalek, J.; Knoll, W. *Anal. Chem.* **2011**, *83*, 6202−6207.
(26) Reiner, A. T.; Fossati, S.; Dostalek, J. *Sens. Actuators, B* **2018**, *257*, 594−601.
(27) Li, W.; Dong, Y.; Wang, X.; Li, H.; Xu, D. *Biosens. Bioelectron.* **2015**, *66*, 43−49.
(28) Wen, J.; Chen, J.; Zhuang, L.; Zhou, S. *Biosens. Bioelectron.* **2016**, *79*, 656−660.
(29) Pei, H.; Li, F.; Wan, Y.; Wei, M.; Liu, H.; Su, Y.; Chen, N.; Huang, Q.; Fan, C. *J. Am. Chem. Soc.* **2012**, *134*, 11876−11879.
(30) Opdahl, A.; Petrovykh, D. Y.; Kimura-Suda, H.; Tarlov, M. J.; Whitman, L. J. *Proc. Natl. Acad. Sci. U.S.A.* **2007**, *104*, 9−14.
(31) Koo, K. M.; Carrascosa, L. G.; Shiddiky, M. J. A.; Trau, M. *Anal. Chem.* **2016**, *88*, 2000−2005.
(32) Koo, K. M.; Carrascosa, L. G.; Shiddiky, M. J. A.; Trau, M. *Anal. Chem.* **2016**, *88*, 6781−6788.
(33) Koo, K. M.; Sina, A. A. I.; Carrascosa, L. G.; Shiddiky, M. J. A.; Trau, M. *Anal. Methods* **2015**, *7*, 7042−7054.
(34) Kimura-Suda, H.; Petrovykh, D. Y.; Tarlov, M. J.; Whitman, L. J. *J. Am. Chem. Soc.* **2003**, *125*, 9014−9015.
(35) Islam, M. N.; Gopalan, V.; Haque, M. H.; Masud, M. K.; Hossain, M. S. A.; Yamauchi, Y.; Nguyen, N.-T.; Lam, A. K.-Y.; Shiddiky, M. J. A. *Biosens. Bioelectron.* **2017**, *98*, 227−233.
(36) Sina, A. A. I.; Carrascosa, L. G.; Palanisamy, R.; Rauf, S.; Shiddiky, M. J. A.; Trau, M. *Anal. Chem.* **2014**, *86*, 10179−10185.
(37) Fang, S.; Lee, H. J.; Wark, A. W.; Corn, R. M. *J. Am. Chem. Soc.* **2006**, *128*, 14044−14046.
(38) Willison, J. R. Signal detection and analysis. *Handbook of Optics Volume I Fundamentals, Techniques, and Design*; Bass, M., Ed.; McGraw-Hill, 1995; Vol. *I*, pp 18.1−18.16.
(39) Lísalová, H.; Brynda, E.; Houska, M.; Víšová, I.; Mrkvová, K.; Song, X. C.; Gedeonová, E.; Surman, F.; Riedel, T.; Pop-Georgievski, O.; Homola, J. *Anal. Chem.* **2017**, *89*, 3524−3531.
(40) Reiner, A. T.; Ferrer, N.-G.; Venugopalan, P.; Lai, R. C.; Lim, S. K.; Dostálek, J. *Analyst* **2017**, *142*, 3913−3921.
(41) Lou, Z.; Han, H.; Zhou, M.; Wan, J.; Sun, Q.; Zhou, X.; Gu, N. *Anal. Chem.* **2017**, *89*, 13472−13479.
(42) Wu, Q.; Sun, Y.; Zhang, D.; Li, S.; Zhang, Y.; Ma, P.; Yu, Y.; Wang, X.; Song, D. *Biosens. Bioelectron.* **2017**, *96*, 288−293.
(43) Springer, T.; Ermini, M. L.; Spackova, B.; Jablonku, J.; Homola, J. *Anal. Chem.* **2014**, *86*, 10350−10356.
(44) Krüger, A.; Bürkle, A.; Mangerich, A.; Hauser, K. *Biomed. Spectrosc. Imaging* **2018**, *7*, 25−33.
(45) Roh, Y. H.; Kim, J. Y.; Mun, S. J.; Lee, H. S.; Hwang, C.; Park, K. H.; Bong, K. W. *Polymers* **2020**, *12*, 546.
(46) Marty, R.; N'soukpoe-Kossi, C. N.; Charbonneau, D.; Weinert, C. M.; Kreplak, L.; Tajmir-Riahi, H.-A. *Nucleic Acids Res.* **2009**, *37*, 849−857.
(47) Wood, B. R. *Chem. Soc. Rev.* **2016**, *45*, 1980.
(48) Lisboa, L. F.; Egli, A.; O'Shea, D.; Åsberg, A.; Hartmann, A.; Rollag, H.; Pang, X. L.; Tyrrell, D. L.; Kumar, D.; Humar, A. *Am. J. Transplant.* **2015**, *15*, 1893−1902.
(49) Chang, Y.-F.; Wang, W.-H.; Hong, Y.-W.; Yuan, R.-Y.; Chen, K.-H.; Huang, Y.-W.; Lu, P.-L.; Chen, Y.-H.; Chen, Y.-M. A.; Su, L.-C.; Wang, S.-F. *Anal. Chem.* **2018**, *90*, 1861−1869.
(50) Hossain, M. Z.; Maragos, C. M. *Biosens. Bioelectron.* **2018**, *101*, 245−252.
(51) Qian, S.; Lin, M.; Ji, W.; Yuan, H.; Zhang, Y.; Jing, Z.; Zhao, J.; Masson, J.-F.; Peng, W. *ACS Sens.* **2018**, *3*, 929−935.
(52) Wei, X.; Duan, X.; Zhou, X.; Wu, J.; Xu, H.; Min, X.; Ding, S. *Analyst* **2018**, *143*, 3134−3140.
(53) Li, J.; Lei, P.; Ding, S.; Zhang, Y.; Yang, J.; Cheng, Q.; Yan, Y. *Biosens. Bioelectron.* **2016**, *77*, 435−441.
(54) Lazzarotto, T.; Blázquez-Gamero, D.; Delforge, M.; Foulon, I.; Luck, S.; Modrow, S.; Leruez-Ville, M. *Front. Pediatr.* **2020**, *8*, 13.
(55) Demmler-Harrison, G. J. *JAMA Pediatr.* **2021**, *175*, No. e205445.

https://doi.org/10.1021/acs.analchem.1c01093
Anal. Chem. 2021, 93, 8002−8009